# Supporting Information

©XMU and CCS

# Selenate Oxyanion Engineering of $RuO_2$ Breaks the Activity–Stability Trade-Off for Acidic Oxygen Evolution

Qisheng Zeng[a,b], Qian Lu[a], Birou Huang[a], Zhuohan Chen[a], Weixing Wu[a], Ying Wang[a,b]*

[a]Department of Chemistry, The Chinese University of HongKong, HongKong 999077, China

[b]Joint Institute of Advanced Materials and Green Energy Research, Great Bay University, Dongguan, Guangdong Province, 523000, P. R. China

E-mail addresses: ying.b.wang@cuhk.edu.hk

ACCEPTED

## Experimental Procedures

### 1.1 Chemicals

$RuCl_3 \cdot H_2O$ (Shanxi Kaida Chemical Engineering Co., Ltd., Ru content ≥ 37.00%); $Na_2SeO_4$ (Aldrich Chemical Co., Inc., purity > 99%); KOH (Aladdin Co., Ltd., ACS); $H_2SO_4$ (RCI Labscan Ltd, purity > 98%); Nafion (DuPont, content > 5%); isopropanol (TEDIA, HPLC/Spectro); Tetramethyl ammonium hydroxide (Aladdin Co., Ltd., AR, 25 wt%.); Methanol (EMD Millipore Corporation, gradient grade); 40% Pt/C (Suzhou Shenernuo Technology Co., Ltd.).

### 1.2 Catalysts synthesis

$SeO_4$-$RuO_2$ was synthesized through a simple two-step procedure consisting of a hydrothermal process followed by calcination. In the first step, 0.2 mmol $RuCl_3 \cdot H_2O$ and 0.02 mmol $Na_2SeO_4$ were dissolved in 15 mL deionized water under stirring. Subsequently, about 33 mg KOH was added to adjust the solution pH to neutral. The resulting homogeneous solution was transferred into 20 mL Teflon-lined stainless-steel autoclave and maintained at 180 ℃ for 5 h. After naturally cooling to room temperature, the precipitate was collected by vacuum filtration and washed several times with deionized water and ethanol, then vacuum-dried. In the second step, the obtained precursor was placed in a crucible and calcined in air at 450 ℃ for 2 h to obtain $SeO_4$-$RuO_2$.

For comparison, the $SeO_4$-$RuO_2$ catalysts with different doping ratio (5%, 20% and 30%) were also prepared using the same synthetic procedure, with the amount of $Na_2SeO_4$ adjusted to 0.01 mmol, 0.04 mmol and 0.06 mmol, respectively. Besides, $RuO_2$ was synthesized through the same procedure without the addition of $Na_2SeO_4$.

### 1.3 Material characterization

The crystal structure of the catalysts was characterized by X-ray diffraction (XRD) using Rigaku SmartLab equipped with Cu $K_\alpha$ radiation ($\lambda$ = 1.5406 Å) operated at 40 kV and 40 mA. XRD patterns were collected over a 2θ range of 20-90° at a scanning rate of 10° $min^{-1}$. The electronic structure of the catalysts was characterized by X-ray photoelectron spectroscopy (XPS) using Thermo Scientific K-Alpha spectrometer equipped with a monochromatic Al $K_\alpha$ X-ray source (hv = 1486.6 eV). All high-resolution XPS spectra were analyzed and fitted using Avantage software. Charge correction was performed by referencing the C 1s peak to a binding energy of 284.8 eV. The morphology and microstructure of the catalysts were characterized using JEOL JEM-F200 transmission electron microscope (TEM). High-solution TEM and energy-dispersive X-ray spectroscopy (EDS) elemental mapping were employed to investigate the lattice structure, crystallinity, and elemental distribution of the catalysts. Raman spectra were collected using HORIBA LabRAM HR Evolution Raman spectrometer equipped with a 633 nm excitation laser to characterize the structural features and vibrational properties of the catalysts. In-situ Fourier transform infrared spectra (FTIR) were collected using Thermo Scientific Nicolet iS50 to monitor the reaction intermediates generated during the oxygen evolution reaction. A background spectrum was first recorded, followed by spectra acquired at the open-circuit potential (OCP) and at applied potentials ranging from 0.7 to 1.6 V vs. RHE with an interval of 0.1 V.

### 1.4 Electrochemical measurement

Electrode preparation: Electrochemical measurements were performed in a standard three-electrode system, using a catalyst-coated glassy carbon electrode (diameter: 3 mm; geometric area: 0.07068 $cm^2$) as the working electrode, a saturated mercurous sulfate electrode as the reference electrode, and a graphite rod as the counter electrode. The working electrode was prepared by dropping the catalyst ink onto the electrode surface and then drying. To prepare the catalyst ink, 5 mg catalyst powder and 2.5 mg carbon black (XC-72R) were dispersed in a mixed solvent containing 400 μL isopropanol, 50 μL deionized water, and 50 μL 5% Nafion D520, followed by ultrasonication for at least 1 h. The catalyst ink was then drop onto the glassy carbon electrode at a loading of 0.25 mg $cm^{-2}$.

ACCEPTED

Electrochemical test: Eletcrochemical measurements were performed in a standard three-electrode system using a CHI760 electrochemical workstation. The oxygen evolution reaction (OER) performance was evaluated in 0.5 M $H_2SO_4$ aqueous electrolyte. Prior to activity measurements, cyclic voltammetry (CV) was performed at a scan rate of 100 mV $s^{-1}$ within the potential range of -0.65 to 0.8 V vs. $Hg/HgSO_4$. for electrode activation. The catalytic activity was then characterized by linear sweep voltammetry (LSV) at a scan rate of 5 mV $s^{-1}$ within the potential range of 0.4 to 1.0 V vs. $Hg/HgSO_4$ by 100% IR compensation. Charge transfer resistance was acquired through electrochemical impedance spectroscopy (EIS) at 0.8 V vs. $Hg/HgSO_4$ with 5 mV AC amplitude over frequency spanning 100 kHz to 100 mHz. All measured potentials were converted to the reversible hydrogen electrode (RHE) scale according to the equation $E_{RHE} = E_{Hg/HgSO4} + 0.652 + 0.059 \times pH$. Catalyst stability was evaluated by chronopotentiometry at a constant current density of 10 mA $cm^{-2}$.

Electrochemical surface area: The electrochemical active surface area (ECSA) was estimated from the electrochemical double-layer capacitance ($C_{dl}$). Cyclic voltammetry (CV) was performed within the non-faradaic potential region (0.10 to 0.20 V vs. $Hg/HgSO_4$) at a scan rate of 10, 20, 30, 40, 50, and 60 mV $s^{-1}$. The $C_{dl}$ was determined from the slope of the linear relationship between $\Delta j/2$ ($\Delta j = j_a - j_c$, $j_a$ and $j_c$ represent the anodic and cathodic current densities measured in the middle potential, respectively) and the scan rates. The ECSA was subsequently calculated according to the equation $ECSA = C_{dl}*A/Cs$, where A is the geometric area of the glassy carbon electrode and the specific capacitance Cs is 0.035 mF $cm^{-2}$.

Stability test: A carbon-paper electrode with an area of 1 × 1 $cm^2$ was used as the working electrode. The catalyst ink was prepared by dispersing 6 mg catalyst powder in a mixture of 900 μL isopropanol, 600 μL deionized water, and 20 μL 5% Nafion D520, followed by ultrasonication. The resulting ink was sprayed onto the carbon paper using an airbrush, with a catalyst loading of 1 mg $cm^{-2}$. A saturated mercurous sulfate electrode and a graphite rod were used as the reference and counter electrodes, respectively. The stability test was conducted in 0.5 M $H_2SO_4$ electrolyte at a constant current density of 10 mA $cm^{-2}$.

ICP-MS analysis and stability number calculation: ICP-MS measurements were conducted using catalyst-coated carbon-paper electrodes with an area of 1 × 1 $cm^2$ and a catalyst loading of 1 mg $cm^{-2}$. A saturated mercurous sulfate electrode and a graphite rod were used as the reference and counter electrodes, respectively. The electrochemical stability test was performed in 40 mL of 0.5 M $H_2SO_4$ at a constant current density of 10 mA $cm^{-2}$. Electrolyte samples (1 mL) were collected at 1, 3, 6, and 10 h using a syringe, and an equal volume of fresh 0.5 M $H_2SO_4$ was subsequently added to maintain a constant electrolyte volume. The collected electrolytes were analyzed by ICP-MS to determine the dissolved Ru and Se concentrations. The stability number (S-number) was calculated according to the equation $S = n_{O2}/n_{dissolved\ Ru}$, where $n_{O2} = Q/(4F)$, $n_{dissolved\ Ru} = (C_{Ru} \times V)/M_{Ru}$, Q is the total charge passed during the 10 h stability test, F is the Faraday constant, $C_{Ru}$ is the dissolved Ru concentration measured by ICP-MS, V is the electrolyte volume, and $M_{Ru}$ is the molar mass of Ru.

**1.5 Water electrolysis**

Membrane electrode assembly (MEA) fabrication: The MEA was fabricated using catalyst-coated membrane (CCM) method. Both anode and cathode catalyst layers were deposited onto the Nafion 212 membrane by spray coating. $SeO_4$-$RuO_2$ and commercial Pt/C (40 wt%) were used as the anode and cathode catalysts, respectively. For the anode catalyst ink: $SeO_4$-$RuO_2$ powder and 5% nafion D520 ionomer (10 wt% relative to the catalyst) were ultrasonically dispersed in a mixed solvent of isopropanol and deionized water (volume ratio = 0.95:0.05) to obtain a catalyst concentration of 5 mg $mL^{-1}$. The cathode catalyst ink was prepared by dispersing commercial Pt/C (40 wt%) and 5% nafion D520 ionomer (10 wt% relative to the catalyst) in a mixed solvent of isopropanol and deionized water (volume ratio = 0.95:0.05) with a catalyst concentration of 5 mg $mL^{-1}$. Both catalyst inks were ultrasonicated for at least 1 h to ensure homogeneous dispersion. Then, spraying the catalyst inks onto both sides of the membrane under heating at 80 ℃ with negative pressure adsorption. Finally, the catalyst-coated membrane was hot-pressed at 135 ℃ under a pressure of 1.5 MPa for 5 min to obtain the MEA. The active area of MEA was 4 $cm^2$, and the catalyst loading was controlled at 2 mg $cm^{-2}$.

Proton exchange membrane water electrolyzer: The electrolyzer was equipped with gold-coated and platinum-coated flow-field plates for the anode and cathode, respectively. Platinum-coated titanium felt was used as the porous transport layer, and the electrolyzer was assembled under a pressure of 1.5 MPa. During electrochemical tests, deionized water was continuously circulated and the operating temperature was maintained at 80 ℃. Electrochemical measurements were performed using a DC power supply. Polarization curves were recorded by applying different current densities, allowing the cell voltage to stabilize before recording. Stability performance was tested under galvanostatic conditions at a current density of 200 mA $cm^{-2}$.

**1.6 Reaction mechanism exploration**

$TMA^+$ molecular probe experiment: To investigate the reaction mechanism, the electrolyte was replaced with 0.5 M $H_2SO_4$ containing 0.1 M $TMA^+$, and the catalyst performance was evaluated in this solution. The electrolyte was prepared as follows: TMAOH was first neutralized with $H_2SO_4$ to pH 7 under continuous stirring. The resulting solution and an appropriate amount of $H_2SO_4$ were then transferred to a volumetric flask, and deionized water was added to volume to obtain the final electrolyte containing 0.1 M $TMA^+$ in 0.5 M $H_2SO_4$. The solution was thoroughly mixed prior to use. Unless otherwise specified, all electrochemical measurements were performed under the same experimental conditions.

Methanol oxidation experiment: The methanol oxidation reaction (MOR) was evaluated in an electrolyte consisting of 0.5 M methanol and 0.5 M $H_2SO_4$. By comparing the linear sweep voltammetry (LSV) curves recorded in 0.5 M $H_2SO_4$ with and without methanol, the intermediate potential region was divided into two parts according to the onset current: a MOR dominated region and a competitive MOR&OER region. The integrated areas of these two regions were then calculated to evaluate the surface *OH coverage and the intrinsic catalytic activity of the catalysts.

pH-dependence experiment: To investigate the deprotonation kinetics of the catalysts, linear sweep voltammetry (LSV) measurements were performed in $H_2SO_4$ electrolytes with different pH values (0.2, 0.4, 0.6, and 0.8), which were precisely adjusted and verified using a pH meter. The reaction order (ρ) was determined from the slope of linear relationship between the logarithm of the current density (at 1.45 V vs. SHE, with iR-compensation) and the pH value.

ACCEPTED

**Supplemental Figures**

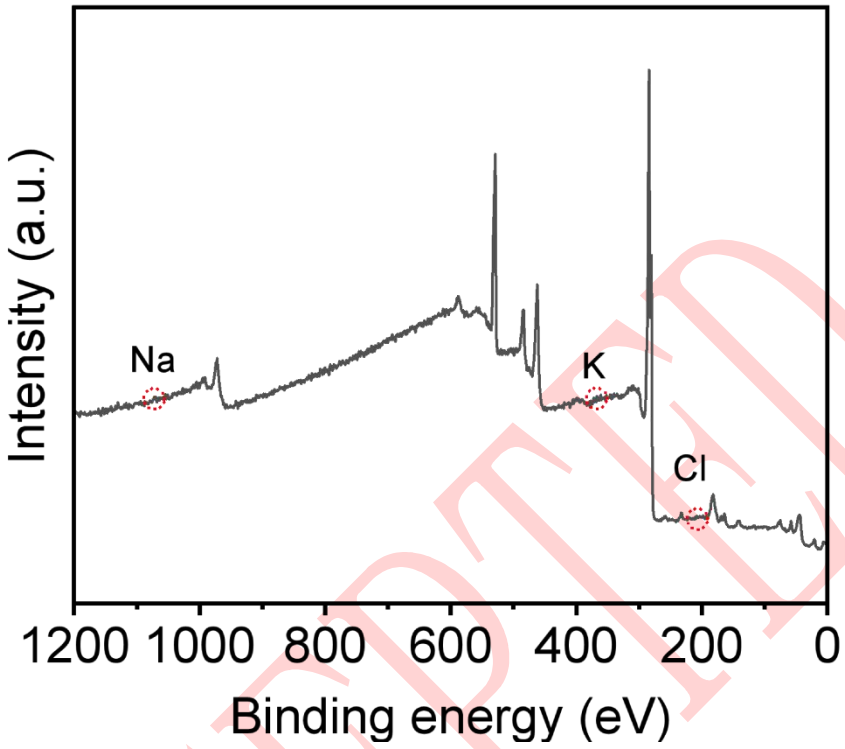



**Figure S1**. XPS survey spectrum for $SeO_4$-$RuO_2$ catalysts.

ACCEPTED

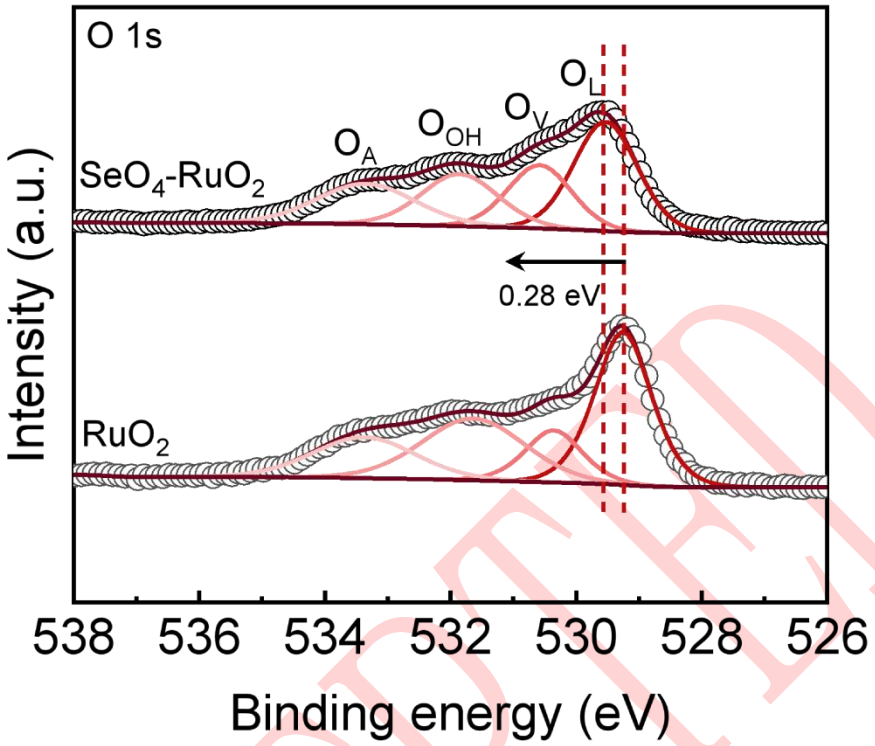



**Figure S2**. High-solution XPS spectra of O 1s for $SeO_4$-$RuO_2$ and $RuO_2$ catalysts, with all spectra calibrated using C 1s at 284.8 eV.

ACCEPTED

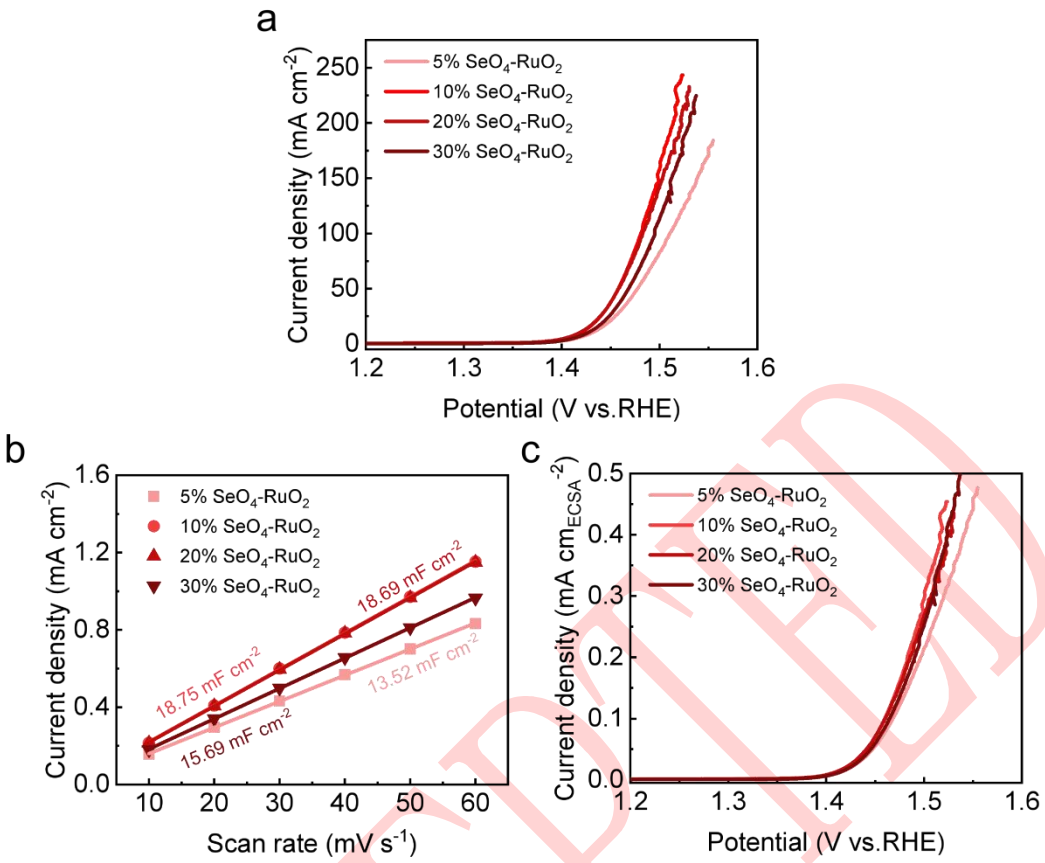



**Figure S3**. (a) OER polarization curves, (b) the double-layer capacitance, and (c) intrinsic activity based on ECSA of x% $SeO_4$-$RuO_2$ catalysts (x = 5, 10, 20, and 30), where x represents the doping ratio.

ACCEPTED

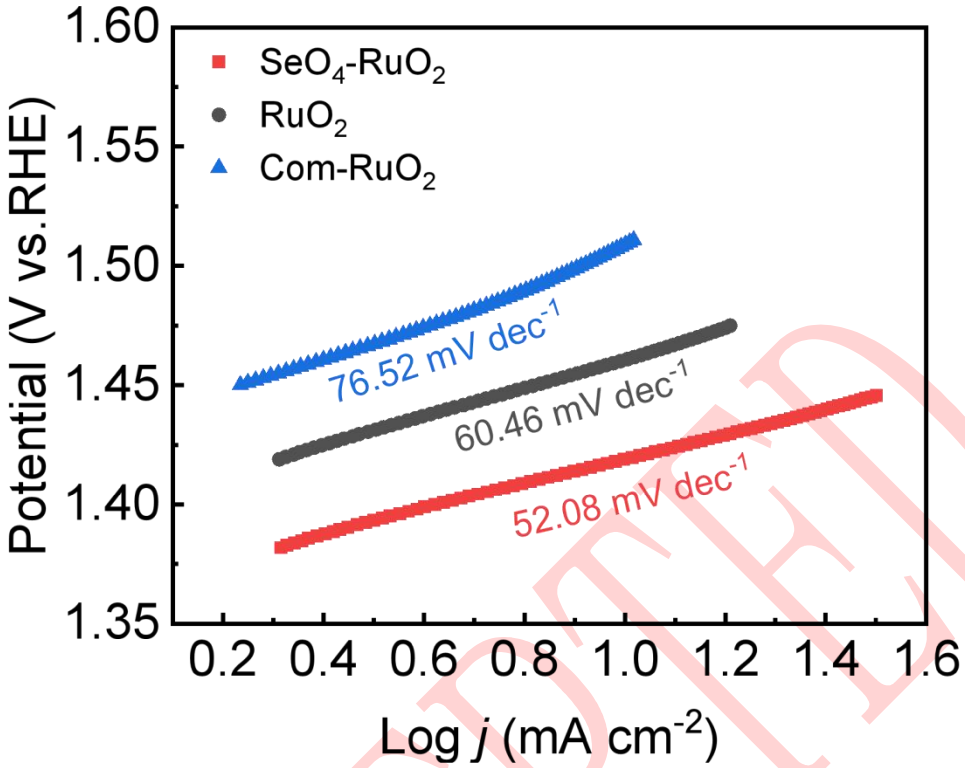



**Figure S4**. Tafel slope of $SeO_4$-$RuO_2$, $RuO_2$ and Com-$RuO_2$ catalysts calculated from OER polarization curves.

ACCEPTED

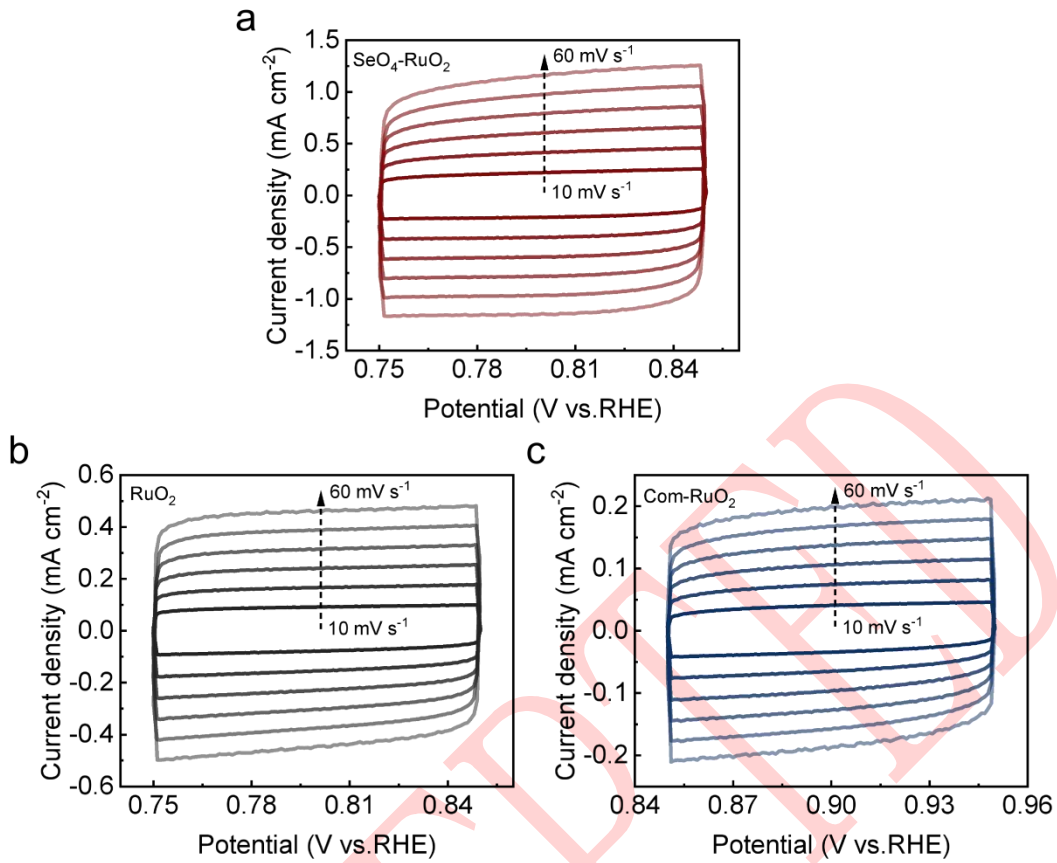



**Figure S5**. CV curves of (a) $SeO_4$-$RuO_2$, (b) $RuO_2$ and (c) Com-$RuO_2$ catalysts.

ACCEPTED

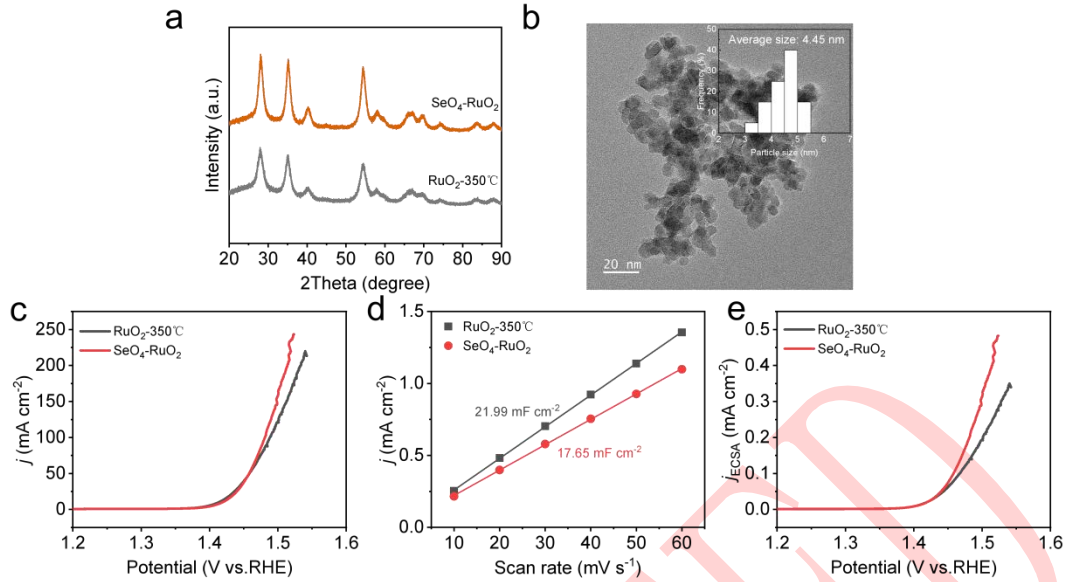



**Figure S6**. (a) XRD patterns of $SeO_4$-$RuO_2$ and $RuO_2$-350℃. (b) TEM image of $RuO_2$-350℃; inset: primary particle size distribution. (c) OER polarization curves of $SeO_4$-$RuO_2$ and $RuO_2$-350℃. (d) Capacitive currents measured at different scan rates and the corresponding double-layer capacitances. (e) Intrinsic OER activities normalized by the ECSA.

ACCEPTED

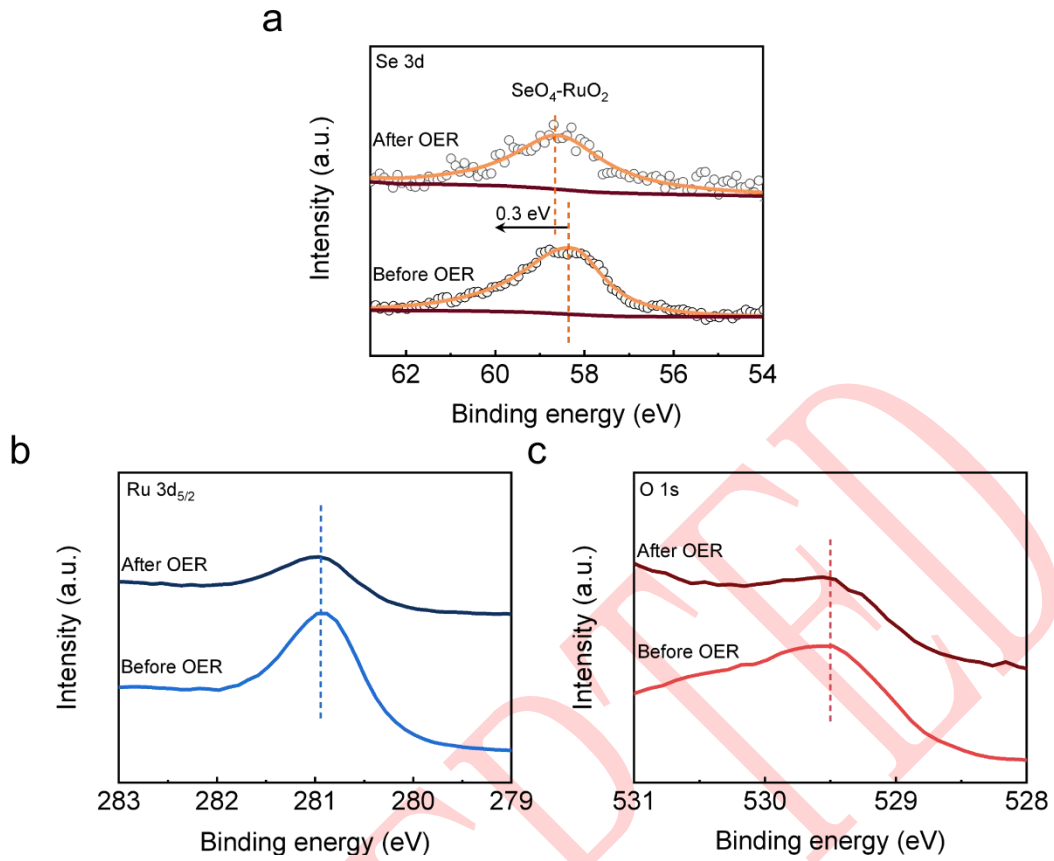



**Figure S7**. High-resolution XPS spectra of (a) Se 3d, (b) Ru $3d_{5/2}$ and (c) O 1s for $SeO_4$-$RuO_2$ catalyst after the OER stability test, with all spectra calibrated using C 1s at 284.8 eV.

ACCEPTED

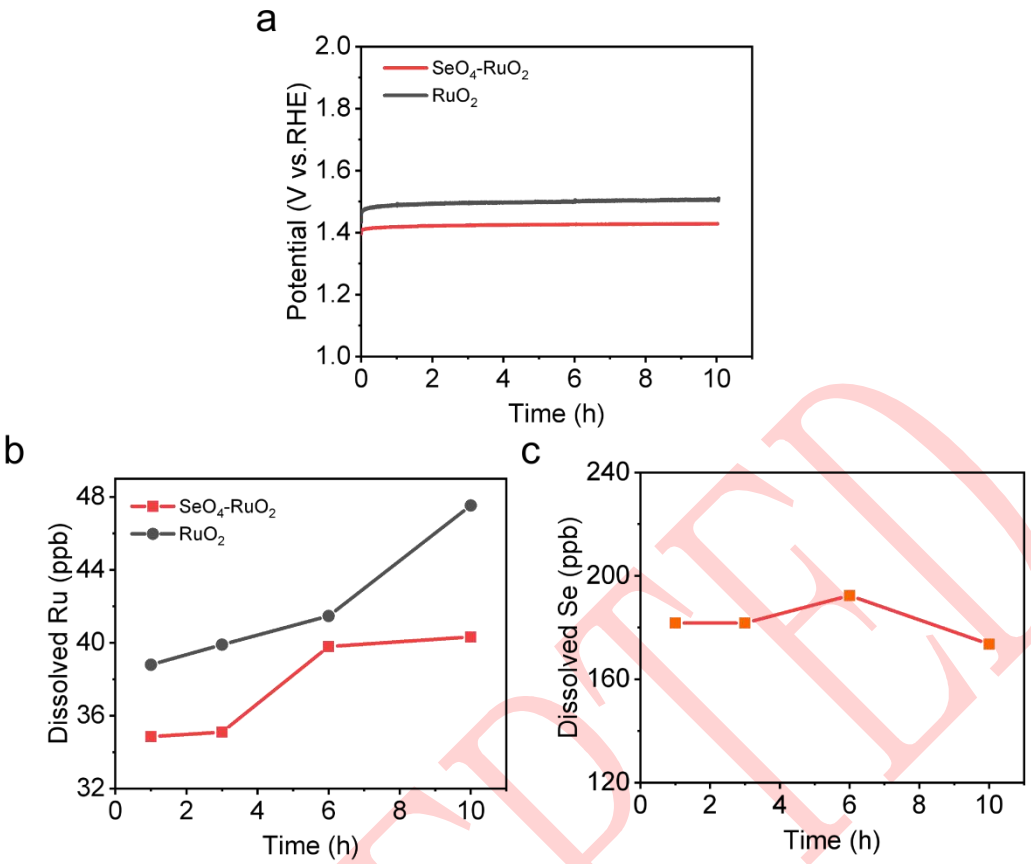



**Figure S8**. (a) Stability test of $SeO_4$-$RuO_2$ and $RuO_2$ at 10 mA $cm^{-2}$. (b) ICP-MS analysis of dissolved Ru for $SeO_4$-$RuO_2$ and $RuO_2$. (c) ICP-MS analysis of dissolved Se for $SeO_4$-$RuO_2$.

ACCEPTED

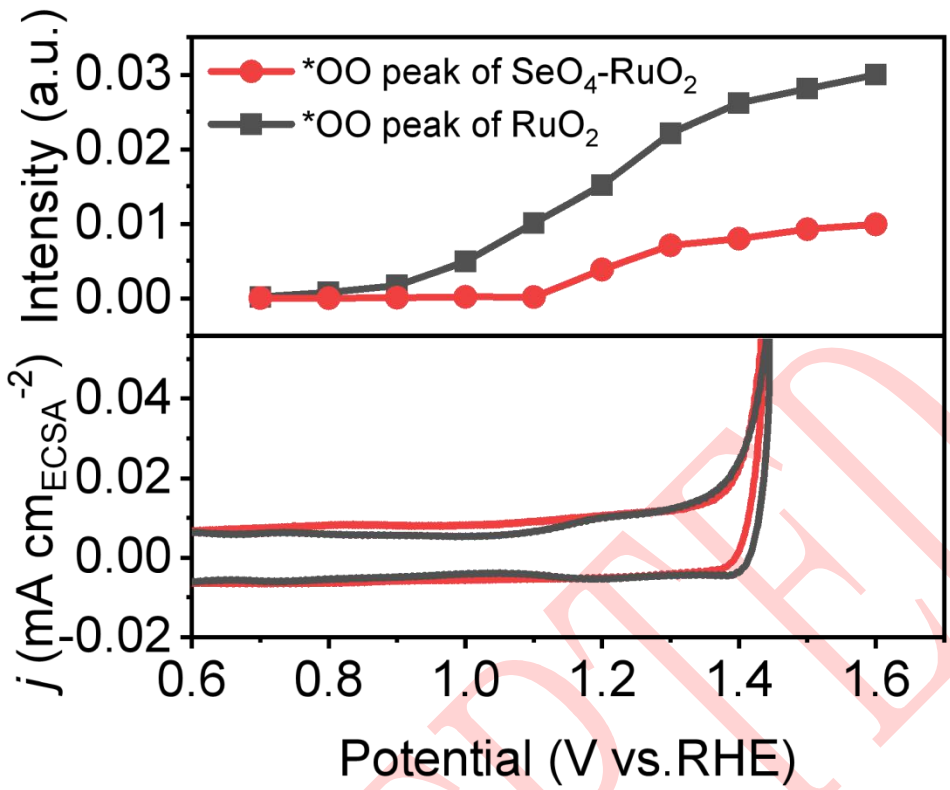



**Figure S9**. Comparison of *OO peak intensity changes and CV curves at different potentials for $SeO_4$-$RuO_2$ and $RuO_2$ catalysts.

ACCEPTED

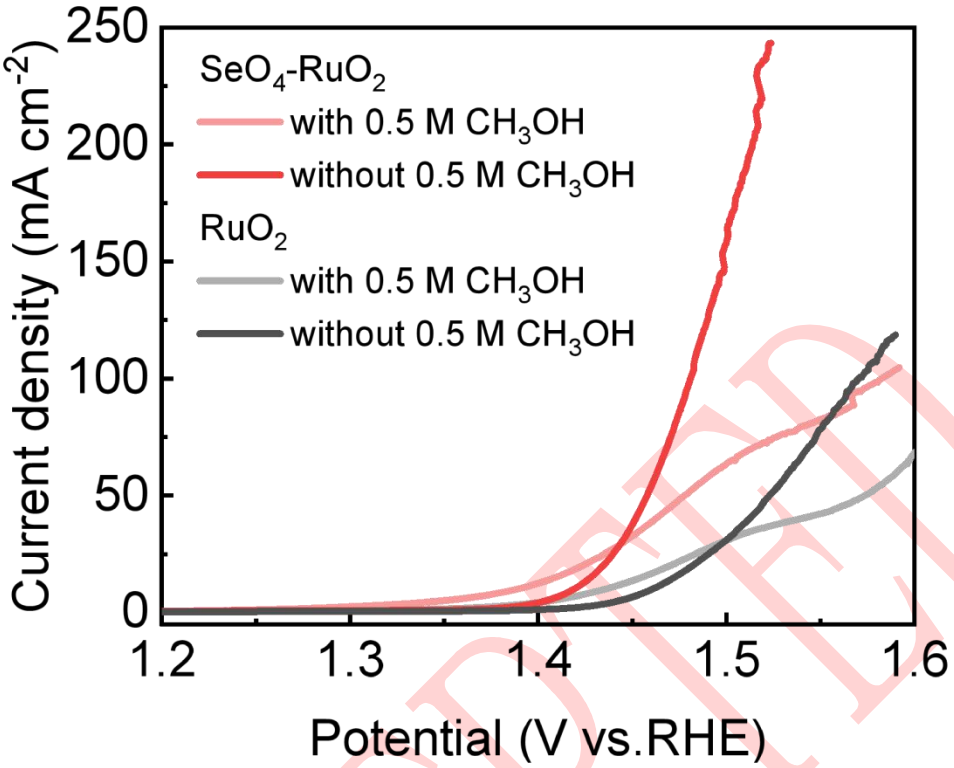



**Figure S10**. OER polarization curves of $SeO_4$-$RuO_2$ and $RuO_2$ catalysts in 0.5 M $H_2SO_4$ with and without 0.5 M $CH_3OH$.

ACCEPTED

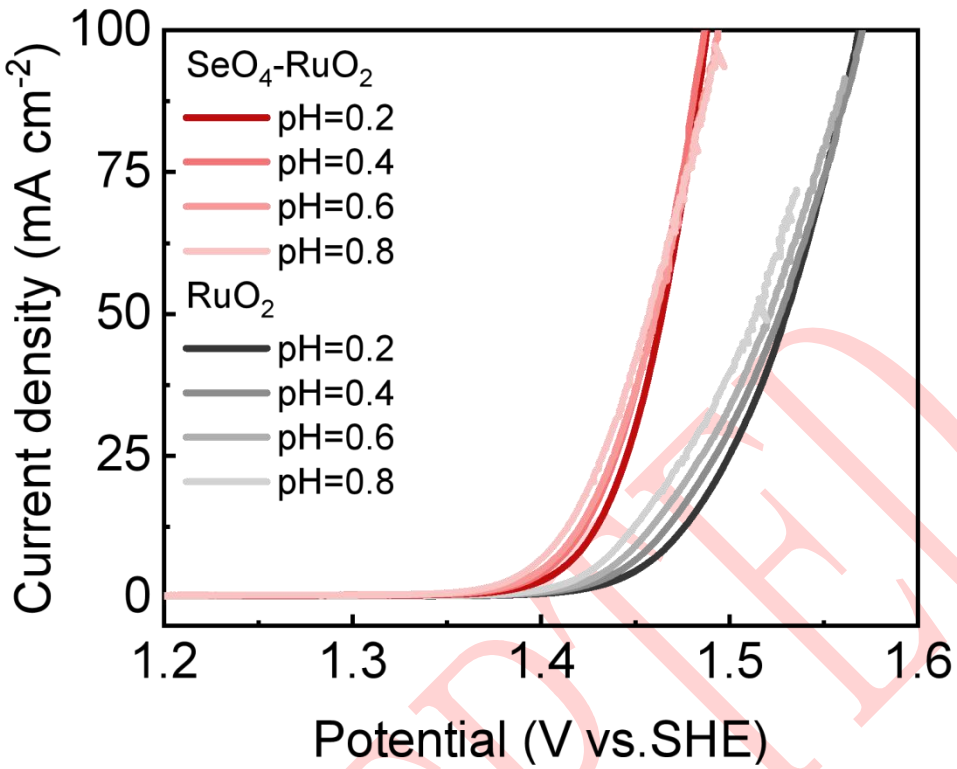



**Figure S11**. OER polarization curves of $SeO_4$-$RuO_2$ and $RuO_2$ catalysts in electrolytes with different pH.

ACCEPTED